POLITECNICO DI TORINO
Repository ISTITUZIONALE

# On the production of chitosan-coated polycaprolactone nanoparticles in a Confined Impinging Jet Reactor

*Original*
On the production of chitosan-coated polycaprolactone nanoparticles in a Confined Impinging Jet Reactor / Zelenková, T.; Mora, M. J.; Barresi, A. A.; Granero, G. E.; Fissore, D.. - In: JOURNAL OF PHARMACEUTICAL SCIENCES. - ISSN 0022-3549. - STAMPA. - 107:4(2018), pp. 1157-1166. [10.1016/j.xphs.2017.11.020]

*Availability:*
This version is available at: 11583/2697229 since: 2020-01-07T17:20:48Z

*Publisher:*
Elsevier

*Published*
DOI:10.1016/j.xphs.2017.11.020

*Terms of use:*

This article is made available under terms and conditions as specified in the corresponding bibliographic description in the repository

*Publisher copyright*
Elsevier postprint/Author's Accepted Manuscript

© 2018. This manuscript version is made available under the CC-BY-NC-ND 4.0 license http://creativecommons.org/licenses/by-nc-nd/4.0/.The final authenticated version is available online at: http://dx.doi.org/10.1016/j.xphs.2017.11.020

(Article begins on next page)

12 October 2024

Journal of Pharmaceutical Sciences [ISSN: 0022-3549], 2018, 17, 1157-1166. DOI: 10.1016/j.xphs.2017.11.020

# On the production of chitosan coated PCL nanoparticles in a Confined Impinging Jets Reactor

Tereza Zelenková[1], Maria Julia Mora[1,2], Antonello A. Barresi[1], Gladys Ester Granero[2], Davide Fissore[1,*]

1. Dipartimento di Scienza Applicata e Tecnologia, Politecnico di Torino, Corso Duca degli Abruzzi 24, 10129 Torino, Italy

2. Departamento de Ciencias Farmacéuticas, Facultad de Ciencias Químicas, Universidad Nacional de Córdoba, Av. Medina Allende y Haya de la Torre, Córdoba, Argentina

* *Corresponding author*
email: davide.fissore@polito.it
tel: 0039-011-0904693

**Abstract**

This work is focused on the synthesis of polycaprolactone nanoparticles, coated with chitosan, in a confined impinging jets reactor using the solvent displacement method. The role of the various reacting species was investigated, evidencing that a biocompatible polymer, e.g. polycaprolactone, is required to support chitosan to obtain a mono-modal particle size distribution, with low particle diameters. A surfactant is required to reduce nanoparticles size (down to a mean diameter of about 260 nm) and obtain a positive Zeta potential (about +31 mV), perfectly suitable for pharmaceutical applications. Different surfactants were tested, and Poloxamer 388 appeared to be preferable to polyvinyl alcohol. The effect of the concentration of Poloxamer 388 (in the range 0.5-5 mg $ml^{-1}$) and of chitosan (in the range 1.5-5 mg $ml^{-1}$) on both the mean particle size and on the Zeta potential was also investigated, evidencing that chitosan concentration has the strongest effect on both parameters. Finally, the effect of solvent evaporation, quenching and feed flow rate was investigated, showing that the evaporation stage does not affect particle characteristics, quenching is required to avoid particle aggregation, and a minimum liquid flow rate of 80 ml $min^{-1}$ is required in the considered reactor to minimize particle size.

**Keyword**

Nanoparticles; nanotechnology; chitosan; particle size; stability; confined impinging jets reactor; solvent displacement.

## Introduction

In the last decades, non-invasive drug administration routes attracted a lot of interest with respect to the traditional parenteral route. In particular, the mucosal route appeared to be a valuable substitute as it allows the drug delivery to the target tissues or to the systemic circulation.[1-3]

In this framework, nanoparticles, with adequate size and surface charge, appeared to be suitable carriers for the mucosal delivery of drugs as they allow protecting drugs from degradation[4], they can be tailored in such a way that the penetration across the mucosal epithelium is improved[5-7] and, finally, the rate of delivery of the drug can be modulated, thus maximizing the efficacy of the drug.[8]

The mucoadhesive properties of the nanoparticles can be improved by coating the nanoparticles by means of mucoadhesive polysaccharides[9,10]: chitosan was extensively used to this purpose as it can interact with the negatively charged mucosal surface and it can open the tight junctions between mucosal cells.[3,11-13] Chitosan is a cationic polysaccharide consisting of β-1 → 4 linked 2-amino-2-deoxy-glucopyranose (GlcN) and 2-acetamido-2-deoxy-β-D-glucopyranose (GlcNAc) residues, produced by deacetylation of chitin, obtained from crustaceans (crabs and shrimps) exoskeleton.[14] Chitosan is characterized by good biodegradability[15], and it exhibits favorable immunostimulating properties[16]. Among the others, Gupta et al. used chitosan to cover polycaprolactone nanoparticles for nasal immunization against influenza A virus.[17] Similarly, Mazzarino et al. covered polycaprolactone nanoparticles containing curcumin for the buccal delivery of this drug[18], while Rampino et al. produced chitosan- tripolyphosphate nanoparticles to deliver various proteins, namely bovine serum albumin, ovalbumin, and human insulin[19].

This paper is focused on the investigation of the synthesis of polycaprolactone (PCL) based nanoparticles coated with chitosan. PCL was used because of its biodegradability and

biocompatibility[20,21]: its degradation products are lactic and glycolic acids and both can be readily eliminated. Besides, PCL is highly stable, and less expensive with respect to other polyesters such as PLGA.

Polymeric nanoparticles were produced using the solvent displacement method as it allows controlling the particle size distribution of the nanoparticles through mixing, and the results are highly reproducible.[22,23] The method requires dissolving firstly the polymer into a solvent and, then, rapidly mixing this solution with an anti-solvent, i.e. a liquid where the polymer is insoluble, thus causing the precipitation of the nanoparticles. Acetone was chosen as polymer solvent, while water was used as anti-solvent.[23]

The mixing of the two streams is obtained in a confined impinging jets reactor (CIJR): two high velocity linear jets of fluid enter the small chamber of the reactor, where highly intense turbulence, resulting in a high mixing efficiency, is obtained. Rapid mixing (the characteristic mixing time is in the order of milliseconds, as evaluated through computational fluid dynamics[24-28]) results into high nucleation rate and, finally, into the formation of very small particles. The production of PCL nanoparticles in the CIJR was investigated by Lince et al.[23,29] and, more recently, by Zelenková et al.[30], focusing on the effect of operating parameters like the liquid flow rate, the ratio between the solvent and the antisolvent flow rates, and the initial polymer concentration on both the mean particle size (and the particle size distribution), and on the Zeta potential of these particles. After nanoparticle synthesis, the nanosuspension is diluted in a certain amount of water with the goal of avoiding particle aggregation and Ostwald ripening[30,31], the so-called “quench” stage, and, finally, the organic solvent is removed through evaporation.

This paper aims investigating the production of PCL nanoparticles, coated by chitosan, in the CIJR: the goal is to produce small size particles, with positive Zeta potential, in such a way that these particles could be used as drug carriers for mucosal delivery. With respect to

particle size, it was reported that trans-epithelial transport of nanoparticles occurs with nanoparticles size ranging from 50 to 100 nm[32]; moreover, nanoparticles with a size of 200 nm or less can be injected intravascularly without the concerns for embolization. On the other hand, for mucosal administration the highest levels of uptake were found with nanoparticles with a ranging size from 100 to 500 nm, while low level of tissue uptake was found for particles with a size of ~1 µm.[33] The effect of the feed composition, as well as of some operating parameters (feed flow rate, solvent evaporation, quench) was investigated by means of an extended experimental investigation.

## Materials and method

Low molecular weight ($M_w$ = 14,000 g mol$^{-1}$) polycaprolactone (PCL) was used for nanoparticle synthesis. All tests were carried out with the same concentration of PCL, namely 5 mg ml$^{-1}$, in acetone (HPLC grade), where the polymer was firstly dissolved. Micro-filtered water (obtained with a Millipore system, Milli-Q RG, Darmstadt, Germany) was used as antisolvent. A surfactant, namely Poloxamer 388 (PEG–PPG–PEG PluronicR-F-108) or polyvinyl alcohol (PVA), was dissolved in the aqueous stream, with a concentration ranging from 0.5 to 5 mg ml$^{-1}$, depending on the goal of the test. All reactants were purchased from Sigma Aldrich (Steinheim, Germany) and used as received.

The confined impinging jets reactor used in this study is shown in Figure 1: it is characterized by a cylindrical mixing chamber with a diameter of 5 mm (with a height of 11.2 mm), and with two inlet pipes with a diameter of 1 mm. Reactants, namely the polymer containing solution and the water stream, are fed to the reactor through a KDS200 syringe pump (KD Scientific, Holliston, USA) and using two plastic syringes with a volume of 100 ml. The experimental apparatus is similar to that used by Zelenková et al.[30,31]. Values of reactants flow rate ranging from 20 to 120 ml min$^{-1}$ were considered in the study, although most of the tests

were carried out at 80 ml $min^{-1}$ as this allowed obtaining smaller nanoparticles. The water to acetone (W/A) flow rate ratio was one in all the tests as mixing conditions are generally jeopardized when this value is different from unity due to the momentum unbalance of the two streams, and to reduction of turbulence intensity when one of the stream flow rate is lower.[30,31]

Low molecular weight chitosan (Sigma-Aldrich, 75-85% deacetylated, with a molecular weight ranging from 50,000 to 190,000 Da, based on viscosity) was used in all the tests. Two different methods of chitosan addition were considered, as sketched in Figure 1: in the first (labelled as #1) chitosan was dissolved in the aqueous stream fed to the CIJR, while in the second (labelled as #2) at first nanoparticles are produced and, then, chitosan is added in such a way that polymeric nanoparticles are used as carriers. In both cases, aiming to dissolve chitosan in water it is necessary to add acetic acid (HPLC grade, Sigma-Aldrich) in such a way that its final concentration was 1%.

Following previous studies[30,31] the stream leaving the reactor was diluted into a certain amount of micro-filtered water: the liquid was then gently stirred, thus allowing the stabilization of the nanoparticle suspension (the “quench”). The ratio between the amount of water used for nanoparticles production and that used for quench is defined quench volumetric ratio: the effect of this parameter was also investigated, considering values in the range 0.1-1.

Finally, after synthesis and quenching, the solvent (acetone) was removed through evaporation in a rotative evaporator (Stuart Rotary Evaporators, Bibby Scientific Ltd., UK): 15 minutes were generally required to completely remove the solvent from a 4 ml sample. In this framework. it has to be taken into account that a small amount of organic solvent may be still present in the final water dispersion, and this could affect particle formation. The role of the solvent in particle formation will be extensively discussed in the followings: in any case, the amount of solvent in the sample after the evaporation stage is expected to be negligible and, thus, it will not affect the particle population obtained in the micro-reactor.

The particle size distribution, as well as the mean size, were measured through Dynamic Light Scattering (DLS Zetasizer Nanoseries ZS90, Malvern Instrument, UK), a technique that allows determining nanoparticles size (z-average) accurately in the range 2 nm - 3 µm. All samples were diluted in water (1:100) before each analysis in order to get reliable measurements, and each measurement was performed in triplicate. The general Mie theory was used to perform the calculations, although the Rayleigh-Gans approximation is valid in the considered system, being the He-Ne laser, used in the Zetasizer, characterized by a wavelength of 633nm. The particle refractive index was assumed to be equal to 1.570 and the particle absorption, imaginary part of the complex index of refraction, was assumed to be equal to 0.010. Although both parameters are not accurately known for the system here considered, being the particle size in the nanometric range, the uncertainty on their values does not significantly affect the obtained results. The Malvern General Purpose non-negative least squares (NNLS) analysis is the algorithm used for calculating the size distribution as it is suitable for the majority of samples where no knowledge of the distribution is available. The Zeta potential, defined as the electrical potential near the particle surface, was determined in the same apparatus, using a special cell equipped with two electrodes. The Henry equation, with Smoluchowsky approximation, was used to get the Zeta potential from the measurement of the electrophoretic mobility.

## Results and discussion

The first part of the experimental investigation was devoted to the study of the effect of the various reactants, namely the PCL, the surfactant (Poloxamer 388) and the chitosan on nanoparticle characteristics, namely the particle size distribution, the mean particle size and the Zeta potential. In this framework, various formulations were investigated: besides nanoparticles containing PCL, Poloxamer 388 and chitosan, also nanoparticles containing only PCL and

chitosan were produced, as well as nanoparticles containing only PCL, only PCL and Poloxamer, and only chitosan, for comparison purposes. Results are shown in Figure 2. Nanoparticles suspensions were obtained in the CIJR using a flow rate of 80 ml $min^{-1}$, with a water to acetone ratio equal to one, and a quench volumetric ratio equal to one, as motivated in the Materials and Methods section. The initial concentration of PCL was equal to 5 mg $ml^{-1}$, while the concentrations of chitosan and of Poloxamer 388 considered in this study were 2.5 mg $ml^{-1}$. Focusing on nanoparticles obtained using only chitosan, it appears that the particles size distribution was not mono-modal (graph a, solid line), with three maxima, indicating that nanoparticles aggregation occurs in the system and, thus, motivating the investigation of the addition of other components in the reacting mixture to improve particle stability. At first, the addition of PCL was considered: particle size distribution (graph a, dotted line) becomes mono-modal, thus indicating that aggregation is no longer occurring, but the mean particle size is too large, about 1000 nm, as shown in graph c, and, thus, these particles are not suitable for pharmaceutical applications, as they are characterized by low level of tissue uptake[33], despite the positive surface potential (shown in graph d) required to fulfill the mucoadhesive function of the particles. Therefore, the addition of a surfactant, namely Poloxamer 388, was considered: also in this case the particle size distribution is mono-modal (graph a, dashed line), thus indicating that nanoparticle aggregation is not occurring, but the mean particle size is now about 260 nm, and the Zeta potential is about +31 mV, thus making these particles perfectly suitable for the pharmaceutical applications. With the goal of formulating a hypothesis on the particles structure, the synthesis of particles containing only PCL and PCL with Poloxamer 388 was investigated. Considering particles composed only of PCL, the mean size was about 200 nm, with a Zeta potential of about -25 mV, as expected. The addition of the surfactant, Poloxamer 388, to the reacting mixture is responsible for a reduction of the mean particle size (to about 180 nm) and for a significant variation of the Zeta potential (to about -10 mV), thus indicating

that part of the surfactant is deposited on the particle surface, with the hydrophobic part oriented towards the interior and the hydrophilic part oriented towards the aqueous medium. When chitosan is added to the reacting mixture, Zeta potential increases and becomes positive (about +31 mV), and the mean particle size increases as well (to about 260 nm), thus indicating that chitosan is located at the particles surface, linked to the hydrophilic part of Poloxamer 388, similarly to what was obtained by Mazzarino et al.[18] using a different production method.

Aiming to investigate the role of the surfactant, i.e. how it influences the mean particle size and the Zeta potential of the nanoparticles, PCL-Poloxamer 388 nanoparticles were produced at constant polymer concentration, equal to 5 mg $ml^{-1}$, and varying the Poloxamer 388 concentration in the feed. Results are shown in Figure 3: it appears that the concentration of Poloxamer 388 has a negligible effect on the mean size of the particles (graph a), while it strongly affects the value of the Zeta potential. In particular, an increase of the value of the Zeta potential is observed in presence of the surfactant (to about -10 mV), independently of its concentration (graph b). This confirms the fact that the surfactant is mainly located at the surface of the particles, and this result can be obtained also in presence of a low concentration of Poloxamer 388. The study has been carried out also in presence of chitosan (at constant concentration, 2.5 mg $ml^{-1}$), and results are shown in Figure 3 for comparison. Also in this case it appears that the concentration of the surfactant does not significantly affect the final mean particle size: taking into account the results shown in Figure 2, graphs a and c, the role of Poloxamer 388 to get small particles is much more important in presence of chitosan and polymer than in presence of the polymer alone. With respect to the effect of the Poloxamer 388 concentration on the particle size and on the Zeta potential, it appears that increasing the surfactant concentration from 0.5 to 1.5 mg $ml^{-1}$ slightly reduces the mean particle size (from about 300 nm to about 250 nm), as it could be expected, but no further reduction of particle size is obtained if the surfactant concentration becomes higher than 1.5 mg $ml^{-1}$. With respect to the

Zeta potential, it appears that increasing the Poloxamer 388 concentration from 0.5 to 1.5 and then to 2.5 mg $ml^{-1}$ results in a decrease of this value, thus confirming the fact that the surfactant is mainly located at the particle surface, where it can replace the chitosan molecules. The value obtained for a Poloxamer 388 concentration equal to 5 mg $ml^{-1}$ is anomalous, probably due to the uncertainty of the experimental measurement of the Zeta potential. Finally, the synthesis of polymer nanoparticles with chitosan, in absence of Poloxamer 388, was investigated, considering different values of chitosan concentration in the reacting medium: results are shown in Figure 3 (graphs c and d). Despite the fact that the values of the Zeta potential obtained were positive (Figure 3, graph d), as requested to obtain a mucoadhesive system, if no surfactant is used the mean particle size becomes very high (Figure 3, graph c) and, thus, these particles should be discarded.

Additional investigation on the role of the surfactant was carried out comparing the results obtained using the Poloxamer 388 with those obtained in presence of a different surfactant, namely the polyvinyl alcohol (PVA): results are shown in Figure 4. In all the tests the same concentration of polymer was considered (5 mg $ml^{-1}$), as well as the same concentration of surfactant (2.5 mg $ml^{-1}$). Tests were carried out with or without chitosan in the reacting mixture: when chitosan was present, its concentration was 2.5 mg $ml^{-1}$. In all cases a mono-modal particle size distribution was observed (Figure 4, graph a), thus pointing out that no aggregation occurred in all cases. With respect to the mean particle size, as shown in graph b, it appears that in absence of chitosan the mean particle size is almost the same, independently on the type of surfactant used; a similar conclusion is gathered considering the Zeta potential shown in graph c. In presence of chitosan, results are strongly different: while in presence of Poloxamer 388 the mean particle size is about 260 nm, when the PVA is used as surfactant it increases to about 450 nm. With respect to the Zeta potential, a mean value of +31 mV is obtained in presence of Poloxamer 388, while a mean value of +55 mV is obtained in presence

of PVA. This means that in presence of PVA there is a larger amount of chitosan covering the external surface of the particles, as it is responsible for both a higher Zeta potential and a larger particle size. Taking into account the desired target of mean particle size, Poloxamer 388 appears to be the preferred surfactant for the case study.

With the goal of understanding how the concentration of chitosan can influence the mean size and the Zeta potential of the PCL-Poloxamer 388-chitosan nanoparticles a set of experiments was carried out varying the concentration of chitosan in the range 1.5-5 mg $ml^{-1}$. The initial PCL concentration was 5 mg $ml^{-1}$, while the concentration of Poloxamer 388 ranged from 0.5 to 5 mg $ml^{-1}$. Results are shown in Figure 5: when the chitosan concentration was increased, also the mean size (graph a) and the Zeta potential (graph b) increased, and the effect of the concentration of Poloxamer 388 was almost negligible in all cases.

Once the role of the different reactants, and of their concentration, was clarified, the influence of the other operating parameters (the way of the nanoparticles production, the solvent evaporation, the feed flow rate and the quench volumetric ratio) on the nanoparticles characteristics was studied.

Firstly, the effect of two different methods (#1) and (#2) of nanoparticles preparation, on the mean size and on the Zeta potential of the nanoparticles was investigated, and results are shown in Figure 6. In all tests, the initial PCL concentration was 5 mg $ml^{-1}$, the concentration of Poloxamer 388 was equal to 5 mg $m^{-1}$ and the concentration of chitosan ranged from 1.5 to 5 mg $ml^{-1}$. It was found that when chitosan was added after the quench and evaporation stages, i.e. with the method #2, the mean particle size was higher (graph a), as well as the Zeta potential (graph b) for all the chitosan concentrations considered in this study. Moreover, in tests #2 particle aggregation was quite often observed, with a multi-modal distribution of particle size. As expected, the mean particle size increased when the chitosan concentration was increased, for both ways of synthesis (graph a). The conclusion that can be gathered from these

experiments is that the way of synthesis #1 has to be preferred to #2.

In order to evaluate the effect of the solvent (acetone) evaporation stage on the mean size and on the Zeta potential of the nanoparticles, both values were measured before and after the evaporation process, as shown in Figure 7, both for PCL-Poloxamer 388 and for PCL-Poloxamer 388-chitosan nanoparticles. The initial concentration of PCL was equal to 5 mg $ml^{-1}$ and that of Poloxamer 388 was equal to 2.5 mg $ml^{-1}$; when chitosan was used, its concentration was 2.5 mg $ml^{-1}$. From the results obtained it appears that the solvent evaporation has a negligible effect on both the mean size and the Zeta potential of the nanoparticles. Similar conclusions can be inferred when PVA, instead of Poloxamer 388, was used as surfactant. Results are shown in Figure 8. The initial concentration of PCL was equal to 5 mg $ml^{-1}$, the concentration of PVA was equal to 2.5 mg $ml^{-1}$ and when chitosan was present its concentration was 2.5 mg $ml^{-1}$. The fact that the nanoparticles characteristics are not influenced by the solvent evaporation is highly positive, because the solvent evaporation stage is essential in the manufacturing process.

With respect to the solvent evaporation stage, a small amount of solvent may be present in the sample after the evaporation stage, originating nanosized organic solvent domains in water that can favor the formation of nanoparticles.[34-38] This phenomenon was evidenced for other systems, but it may occur also in acetone-water mixtures, as it was evidenced both experimentally[39] and using molecular dynamics simulation[40,41]. In particular, using molecular dynamics it was demonstrated that even if water and acetone are perfectly miscible, an appreciable segregation of the two solvents may occur at nanometric scale, being it maximum when the acetone fraction is 0.5. This affects the nucleation rate in the micro-reactor. With respect to the solvent evaporation stage, it was designed in such a way that all the acetone is removed: this was confirmed by weighing samples before and after this stage. Obviously, only very small amount of acetone could remain in the system and, thus, the additional nanoparticle

formation that may take place in these domains is expected to be negligible. This was confirmed by evaluating the evolution of nanoparticle population vs. time (results not shown in this paper for the sake of brevity) where the particle size distribution appeared not to change even after 2 months.

One of the parameters that can affect the size of the nanoparticles produced in the CIJR is the liquid flow rate. Previous experiments were carried out at 80 ml $min^{-1}$, since it is known that the high flow rates ensure the best mixing condition during the nanoprecipitation process. For sake of completeness, the influence of the flow rate on the mean particle size and on the Zeta potential was investigated in the range 20-120 ml $min^{-1}$ and results are shown in Figure 9. As it is expected from previous studies[30,28,42] when the flow rate is increased the mean size of the nanoparticle decreases. Although no general agreement on the process of particle formation can be found in the literature, Computational Fluid Dynamics was used to clarify the role of various operating parameters and, in particular, also of the feed flow rate.[43,26] Mixing, particle nucleation and growth were demonstrated to occur in series, while particle aggregation occurs in parallel with growth. Mixing strongly affects the local supersaturation, and, thus, also particle nucleation (strongly), growth (weakly) and aggregation. Therefore, smaller particles are obtained when mixing is improved (as a consequence of the higher flow rate) due to higher nucleation rate. The same conclusion is obtained in case particle formation by self-assembly is assumed: in fact, the size of the nanoparticles is proportional to the ratio of mixing and coalescence, but the expression used for nucleation can still be used to approximate the process.[44] After exceeding a limit value, in this case study 80 ml $min^{-1}$, the mean size of nanoparticles did not further decrease significantly, and the size remained practically constant. Similar trend was also observed for the Zeta potential: with increasing the liquid flow rate the values of the Zeta potential became smaller, and at high levels of flow rate (> 80 ml $min^{-1}$) it remained constant at around +30 mV.

Since it is known that the quantity of water used for the quenching can significantly affect the mean size of nanoparticles obtained through the CIJR[30], a set of experiments was carried out varying the quench volumetric ratio from 0.125 to 1. Taking into account the definition of this parameter, when the ratio is equal to 1 it means that the amount of water used for the quench is exactly the same used for the synthesis (as antisolvent), while in case the ratio is 0.125 it means that the amount of water used for the quench is 8 times that used for the synthesis (and, thus, the final dilution is higher). Results are shown in Figure 10 with respect to both the mean particle size and the Zeta potential. A test without quench was also carried out: in this case the mean particle size resulted to be equal to 377±87 nm, while values around 270 nm are obtained when quench is used in the manufacturing stage. It can thus be stated that the quench is essential to get smaller nanoparticles, but the excess of water used for quench plays an insignificant role regarding the nanoparticles mean size, as shown in graph a. Similar conclusion can be gathered with respect to the Zeta potential, as it is shown in graph b: a decrease in the Zeta potential when increasing the quantity of water used for the quench was in fact observed.

## Conclusions

The feasibility of the production of chitosan coated PCL nanoparticles in the confined impinging jets reactor, using the solvent displacement method, was demonstrated by means of an extended experimental investigation. Small size nanoparticles (about 250 nm mean diameter) with a positive Zeta potential (about +30 mV), required to have mucoadhesive characteristics, are obtained using polycaprolactone, in presence of a surfactant (Poloxamer 388). The high value of the Zeta potential suggests that these particles are highly stable, i.e. no aggregation is expected to occur, when stored in solution and where used, even at physiologic ionic strength. Better results are obtained feeding chitosan with the anti-solvent (water) stream,

instead of adding it after nanoparticle synthesis. Chitosan concentration has the strongest effect on nanoparticle size and Zeta potential. With respect to the manufacturing process, the solvent evaporation stage has a negligible effect on both the mean particle size and the Zeta potential, while quench is required to avoid particle aggregation, but results are scarcely affected by the amount of water used for quench. Future investigations will focus on the encapsulation of a test drug in the nanoparticles produced through this way, and on the study of the release of this drug.

**Acknowledgement**

Financial support of the Bilateral Cooperation Project between Italy and Argentina (AR14MO8) is gratefully acknowledged. The authors would like to thank Daniela Falcone for her contribution to the experimental investigation.

## List of symbols

| | |
|---|---|
| $c_{Chi}$ | chitosan concentration, mg ml$^{-1}$ |
| $c_{PCL}$ | polymer concentration, mg ml$^{-1}$ |
| $c_{Pol388}$ | Poloxamer 388 concentration, mg ml$^{-1}$ |
| $c_{PVA}$ | polyvinyl alcohol concentration, mg ml$^{-1}$ |
| $d_p$ | particle diameter, nm |
| $M_w$ | molecular weight, kg kmol$^{-1}$ |

*Abbreviations*

| | |
|---|---|
| CIJR | Confined Impinging Jets Reactor |
| FR | Flow rate, ml min$^{-1}$ |
| PCL | Polycaprolactone |
| W/A | Water to Acetone ratio |

**List of references**


1. Huang Y, Leobandung W, Foss A, Peppas NA. Molecular aspects of muco- and bioadhesion: tethered structures and site-specific surfaces. *J Control Release*. 2000;65(1-2):63-71.
2. Chowdary KP, Rao YS. Mucoadhesive microspheres for controlled drug delivery. *Biol Pharm Bull*. 2004;27(11):1717-1724.
3. Andrews GP, Laverty TP, Jones DS. Mucoadhesive polymeric platforms for controlled drug delivery. *Eur J Pharm Biopharm*. 2009;71(3):505–518.
4. Des Rieux A, Fievez V, Garinot M, Schneider YJ, Préat V. Nanoparticles as potential oral delivery systems of proteins and vaccines: a mechanistic approach. *J Control Release*. 2006;116(1):1–27.
5. Lamprecht A, Schafer U, Lehr CM. Size-dependent bioadhesion of micro-and nanoparticulate carriers to the inflamed colonic mucosa. *Pharm Res*. 2001;18(6):788–793.
6. Prego C, Garcia M, Torres D, Alonso MJ. Transmucosal macromolecular drug delivery. *J Control Release*. 2005;101(1-3):151–162.
7. Pathan SA, Iqbal Z, Sahani JK, Talegaonkar S, Khar RK, Ahmad FJ. Buccoadhesive drug delivery systems-extensive review on recent patents. *Recent Pat Drug Deliv Formul*. 2008;2(2):177-188.
8. Kammona O, Kiparissides C. Recent advances in nanocarrier-based mucosal delivery of biomolecules. *J Control Release*. 2012;161(3):781–794.
9. Lemarchand C, Gref R, Couvreur P. Polysaccharide-decorated nanoparticles. *Eur J Pharm Biopharm*. 2004;58(2):327-341.
10. Liu Z, Jiao Y, Wang Y, Zhou C, Zhang Z. Polysaccharides-based nanoparticles as drug

delivery systems. *Adv Drug Deliv Rev*. 2008;60(15):1650-1662.

11. Lehr CM, Bouwstra JA, Schacht EH, Junginger HE. In vitro evaluation of mucoadhesive properties of chitosan and some other natural polymers. *Int J Pharm*. 1992;78(1-3):43–48.
12. Issa M, Koping-Hoggard M, Artursson P. Chitosan and the mucosal delivery of biotechnology drugs. *Drug Discov Today Technol*. 2005;2(1):1–6.
13. Dash M, Chiellini F, Ottenbrite RM, Chiellini E. Chitosan-A versatile semi-synthetic polymer in biomedical applications. *Progr Polym Sci*.2011;36(8):981–1014.
14. Tømmeraas K, Köping-Höggård M, Vårum KM, Christensen BE, Artursson P, Smidsrød O. Preparation and characterisation of chitosans with oligosaccharide branches. *Carbohydr Res*. 2002;337(24):2455–2462.
15. Lee KY, Ha SW, Park WH. Blood biocompatibility and biodegradability of partially N-acylated chitosan derivatives. *Biomaterials*. 1995;16(16):1211–1216.
16. Nishimura K, Ishihara C, Ukei S, Tokura S, Azuma I. Stimulation of cytokine production in mice using deacetylated chitin. *Vaccine*. 1986;4(3):151–156.
17. Gupta NK, Tomar P, Sharma V, Dixit VK. Development and characterization of chitosan coated poly-(ε-caprolactone) nanoparticulate system for effective immunization against influenza. *Vaccine*. 2011;29(48):9026-9037.
18. Mazzarino L, Travelet C, Ortega-Murillo S, Otsuka I, Pignot-Paintrand I, Lemos-Senna E, Borsali R. Elaboration of chitosan-coated nanoparticles loaded with curcumin for mucoadhesive applications. *J Colloid Interface Sci*. 2012;370(1):58-66.
19. Rampino A, Borgogna M, Blasi P, Bellich B, Cesàroa A. Chitosan nanoparticles: Preparation, size evolution and stability. *Int J Pharm*. 2013;455(1-2):219– 228.
20. Alonso MJ, 1996. Nanoparticulate drug carrier technology, in: Cohen S, Bernstein H, (Eds.), Microparticulate Systems for the Delivery of Proteins and Vaccines. Marcel

Dekker, New York, pp. 203–242.

21. Sinha VR, Bansal K, Kaushik R, Kumria R, Trehan A. Poly-ε-caprolactone microspheres and nanospheres: an overview. *Int J Pharm*. 2004;278(1):1-23.

22. Horn D, Rieger J, 2001. Organic nanoparticles in the aqueous phase - theory, experiment, and use. *Angew Chem Int Ed Engl*. 2001;40(23):4330-4361.

23. Lince F, Marchisio DL, Barresi AA. Strategies to control the particle size distribution of poly-*ε*-caprolactone nanoparticles for pharmaceutical applications. *J Colloid Int Sci.* 2008;322(2):505–515.

24. Marchisio DL, Rivautella L, Barresi AA. Design and scale-up of chemical reactors for nanoparticle precipitation. *AIChE J.* 2006;52(5):1877-1887.

25. Gavi E, Rivautella L, Marchisio DL, Vanni M, Barresi AA, Baldi G. CFD modelling of nano-particle precipitation in confined impinging jet reactors. *Chem Eng Res Des.* 2007;85(5):735-744.

26. Lince F, Marchisio DL, Barresi AA. A comparative study for nanoparticle production with passive mixers via solvent-displacement: Use of CFD models for optimization and design. *Chem Eng Proc*. 2011;50(4):356-368.

27. Di Pasquale N, Marchisio DL, Barresi AA. Model validation for precipitation in solvent-displacement processes. *Chem Eng Sci*. 2012;84:671-683.

28. Barresi AA, Vanni M, Fissore D, Zelenková T, 2015. Synthesis and preservation of polymer nanoparticles for pharmaceuticals applications. In: Handbook of Polymers for Pharmaceutical Technologies: Processing and Applications, Volume 2 (Thakur VK, Thakur MK, editors), pp. 229-280.

29. Lince F, Marchisio DL, Barresi AA. Smart mixers and reactors for the production of pharmaceutical nanoparticles: Proof of concept. *Chem Eng Res Des*. 2009;87(4):543–549.

30. Zelenková T, Fissore D, Marchisio DL, Barresi AA. Size control in production and freeze-drying of poly-ε-caprolactone nanoparticles. *J Pharm Sci*. 2014;103(6):1839-1850.

31. Zelenková T, Barresi AA, Fissore D. On the use of tert-butanol/water co-solvent systems in production and freeze-drying of poly-ε-caprolactone nanoparticles. *J Pharm Sci*. 2015;104(1):178-190.

32. He Z, Santos JL, Tian H, Huang H, Hu Y, Liu L, Leong KW, Chen Y, Mao HQ. Scalable fabrication of size-controlled chitosan nanoparticles for oral delivery of insulin. *Biomaterials*. 2017;130:28-41.

33. Hickey JW, Santos JL, Williford JM, Mao HQ. Control of polymeric nanoparticle size to improve therapeutic delivery. *J Control Release*. 2015;219:536-547.

34. Stancanelli R, Guardo M, Cannavà C, Gugliemo G, Ficarra P, Villari V, Micali N, Mazzaglia A. Amphiphilic cyclodextrins as nanocarriers of genistein: A spectroscopic investigation pointing out the structural properties of the host/drug complex system. *J Pharm Sci*. 2010;99(7):3141-3149.

35. Micali N, Vybornyi M, Mineo P, Khorev O, Haner R, Villari V. Hydrodynamic and thermophoretic effects on the supramolecular chirality of pyrene-derived nanosheets. *Chem Eur J*. 2015;21:9505-9513.

36. Stancanelli R, Loikner LD, Larsen KL, Guardo M, Cannavà C, Tommasini S, Ventura CA, Calabrò ML, Micali N, Villari V, Mazzaglia A. Structural and spectroscopic features of lutein/butanoyl-β-cyclodextrin nanoassemblies. *J Pharm Biom Anal*. 2012;71:214-218.

37. Sedlak M. Large-scale supramolecular structure in solutions of low molar mass compounds and mixtures of liquids: I. Light scattering characterization. *J Phys Chem B.* 2006,110(9),4329-4338

38. Sedlak M. Large-scale supramolecular structure in solutions of low molar mass compounds and mixtures of liquids: II. Kinetics of the formation and long-time stability. *J Phys Chem B*. 2006,110(9),4339-4345.

39. Matteoli E, Lepori L. Solute–solute interactions in water. II. An analysis through the Kirkwood–Buff integrals for 14 organic solutes. J Chem Phys. 1984;80(6):2856-2863.

40. Weerasinghe S, Smith PE. Kirkwood-buff derived force field for mixtures of acetone and water. *J Chem Phys*. 2003;118(23):10663−10670.

41. Di Pasquale N, Marchisio DL, Barresi AA, Carbone P. Solvent structuring and its effect on the polymer structure and processability: The case of water-acetone poly-ε-caprolactone mixtures. J Phys Chem B. 2014;118(46):13258–13267.

42. Ferri A, Kumari N, Peila R, Barresi AA. Production of menthol-loaded nanoparticles by solvent displacement. *Canad J Chem Eng*. 2017;95(9):1690-1706.

43. Liu Y, Cheng C, Liu Y, Prud'homme RK, Fox RO. Mixing in a multi-inlet vortex mixer (MIVM) for flash nano-precipitation. *Chem Eng Sci*. 2008;63(11):2829-2842.

44. Lavino AD, Di Pasquale N, Carbone P, Marchisio DL. A novel multiscale model for the simulation of polymer flash nano-precipitation. *Chem Eng Sci*. 2017;171:485-494.

**List of Figures**

**Figure 1.** Experimental apparatus used for the nanoparticle synthesis using the solvent displacement method in the CIJR (the infusion pumps and the mixer are evidenced in the picture) and sketch of the two routes (labelled as #1 and #2) for nanoparticles synthesis used in this study.

**Figure 2.** Particle size distribution (graphs a and b), mean particle size (graph c) and Zeta potential (graph d) obtained for various feed compositions (operating conditions: FR = 80 ml min$^{-1}$, W/A = 1, quench volumetric ratio = 1):

(A) $c_{Chi}$ = 2.5 mg ml$^{-1}$ (graph a, solid line);

(B) $c_{PCL}$ = 5 mg ml$^{-1}$, $c_{Chi}$ = 2.5 mg ml$^{-1}$ (graph a, dotted line);

(C) $c_{PCL}$ = 5 mg ml$^{-1}$, $c_{Chi}$ = 2.5 mg ml$^{-1}$, $c_{Pol\ 388}$ = 2.5 mg ml$^{-1}$ (graph a, dashed line);

(D) $c_{PCL}$ = 5 mg ml$^{-1}$ (graph b, solid line);

(E) $c_{PCL}$ = 5 mg ml$^{-1}$, $c_{Pol\ 388}$ = 2.5 mg ml$^{-1}$ (graph b, dashed line).

**Figure 3.** Influence of the concentration of Poloxamer 388 on the mean particle size (graph a) and on the Zeta potential (graph b) in case of nanoparticles produced using PCL($c_{PCL}$ = 5 mg ml$^{-1}$) (■) and using using PCL ($c_{PCL}$ = 5 mg ml$^{-1}$) and chitosan ($c_{Chi}$ = 2.5 mg ml$^{-1}$) (▲) and influence of chitosan on the mean particle size (graph c) and on the Zeta potential (graph d) in case of nanoparticles produced using PCL ($c_{PCL}$ = 5 mg ml$^{-1}$) (operating conditions: FR = 80 ml min$^{-1}$, W/A = 1, quench volumetric ratio = 1).

**Figure 4.** Influence of chitosan on particle size distribution (graph a), mean particle size (graph b) and Zeta potential (graph c) in presence of different surfactants (operating conditions: FR = 80 ml min$^{-1}$, W/A = 1, quench volumetric ratio = 1):

(A) $c_{PCL}$ = 5 mg ml$^{-1}$, $c_{Pol\ 388}$ = 2.5 mg ml$^{-1}$ (dash-dotted line, □);

(B) $c_{PCL}$ = 5 mg ml$^{-1}$, $c_{PVA}$ = 2.5 mg ml$^{-1}$ (solid line, ■);

(C) $c_{PCL}$ = 5 mg ml$^{-1}$, $c_{Chi}$ = 2.5 mg ml$^{-1}$, $c_{Pol\ 388}$ = 2.5 mg ml$^{-1}$ (dashed line, ▨);

(D) $c_{PCL}$ = 5 mg ml$^{-1}$, $c_{Chi}$ = 2.5 mg ml$^{-1}$, $c_{PVA}$ = 2.5 mg ml$^{-1}$ (dotted line, ▥);

**Figure 5.** Effect of the concentration of Poloxamer 388 (A: $c_{Pol\ 388}$ = 0.5 mg ml$^{-1}$, B: $c_{Pol\ 388}$ = 1.5 mg ml$^{-1}$, C: $c_{Pol\ 388}$ = 2.5 mg ml$^{-1}$, D: $c_{Pol\ 388}$ = 5 mg ml$^{-1}$) and of chitosan (grey bar: $c_{Chi}$ = 1.5 mg ml$^{-1}$, light grey bar: $c_{Chi}$ = 2.5 mg ml$^{-1}$, white bar: $c_{Chi}$ = 5 mg ml$^{-1}$) on the mean particle size (graph a) and on the Zeta potential (graph b) of nanoparticles produced using PCL ($c_{PCL}$ = 5 mg ml$^{-1}$) (operating conditions: FR = 80 ml min$^{-1}$, W/A = 1, quench volumetric ratio = 1).

**Figure 6.** Effect of the concentration of chitosan on mean particle size (graph a), and Zeta potential (graph b) in case of nanoparticles produced using PCL ($c_{PCL}$ = 5 mg ml$^{-1}$, $c_{Pol\ 388}$ = 5 mg ml$^{-1}$) produced using the method #1 (dashed lines, □) or the method #2 (solid lines, ■)

**Figure 7.** Comparison of the mean particle size (graph a) and of the Zeta potential (graph b) of nanoparticles composed of PCL ($c_{PCL}$ = 5 mg ml$^{-1}$) and Poloxamer 388 ($c_{Pol\ 388}$= 2.5 mg ml$^{-1}$), without (A) or with (B) chitosan ($c_{Chi}$ = 2.5 mg ml$^{-1}$) before (□) and after (■) the evaporation. (operating conditions: FR = 80 ml min$^{-1}$, W/A = 1, quench volumetric ratio = 1).

**Figure 8.** Comparison of the mean particle size (graph a) and of the Zeta potential (graph b) of nanoparticles composed of PCL ($c_{PCL}$ = 5 mg ml$^{-1}$) and PVA ($c_{PVA}$ = 2.5 mg ml$^{-1}$), without (A)

or with (B) chitosan ($c_{Chi}$ = 2.5 mg ml$^{-1}$) before (□) and after (■) the evaporation (operating conditions: FR = 80 ml min$^{-1}$, W/A = 1, quench volumetric ratio = 1).

**Figure 9.** Influence of the liquid flow rate on the mean particle size (graph a) and on the Zeta potential (graph b) of nanoparticles composed of PCL ($c_{PCL}$ = 5 mg ml$^{-1}$), Poloxamer 388 ($c_{Pol\ 388}$ = 2.5 mg ml$^{-1}$) and chitosan ($c_{Chi}$ = 2.5 mg ml$^{-1}$) (operating conditions: W/A = 1, quench volumetric ratio = 1).

**Figure 10.** Influence of the quench volumetric ratio on the mean particle size (graph a) and on the Zeta potential (graph b) of nanoparticles composed of PCL ($c_{PCL}$ = 5 mg ml$^{-1}$), Poloxamer 388 ($c_{Pol\ 388}$ = 2.5 mg ml$^{-1}$) and chitosan ($c_{Chi}$ = 2.5 mg ml$^{-1}$) (operating conditions: FR = 80 ml min$^{-1}$, W/A = 1).

*Figure 1*

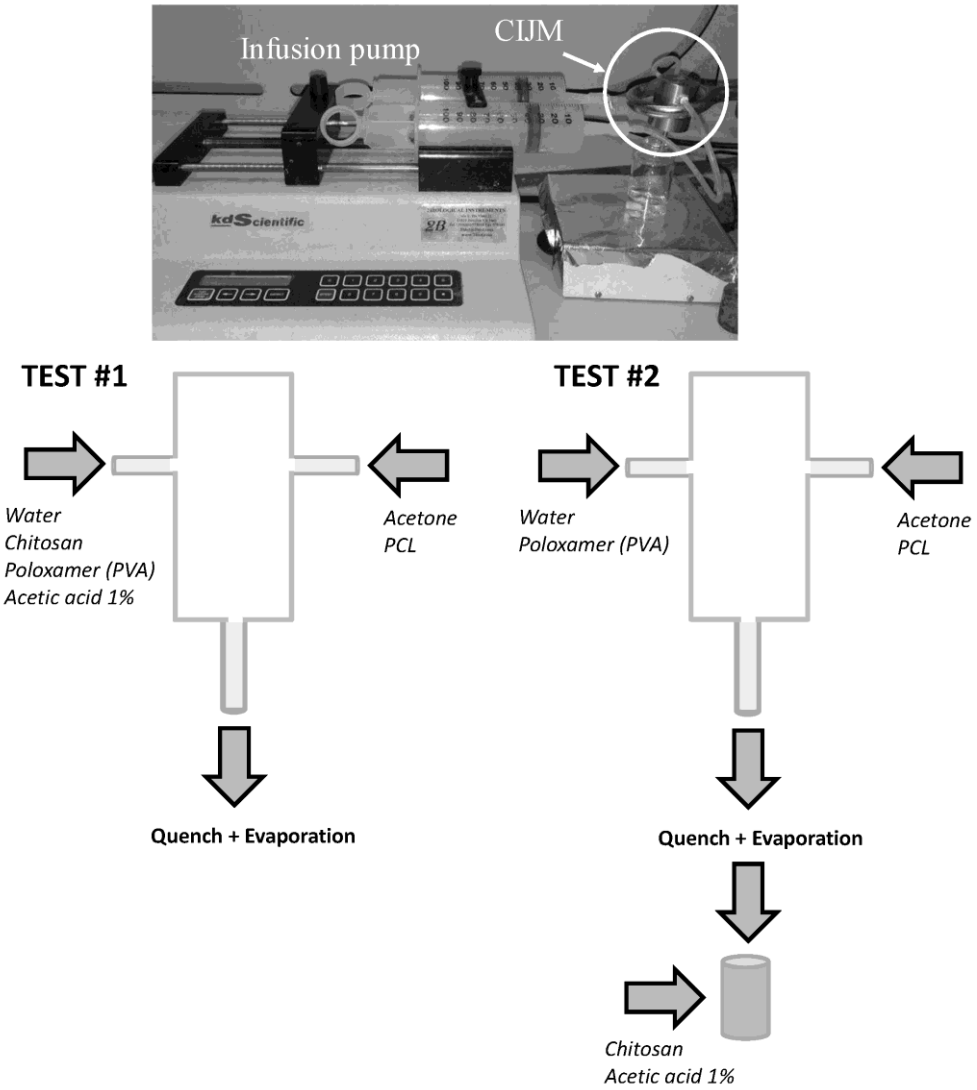
Infusion pump
CIJM
kdScientific
TEST #1
Water
Chitosan
Poloxamer (PVA)
Acetic acid 1%
Acetone
PCL
Quench + Evaporation
TEST #2
Water
Poloxamer (PVA)
Acetone
PCL
Quench + Evaporation
Chitosan
Acetic acid 1%

*Figure 2*

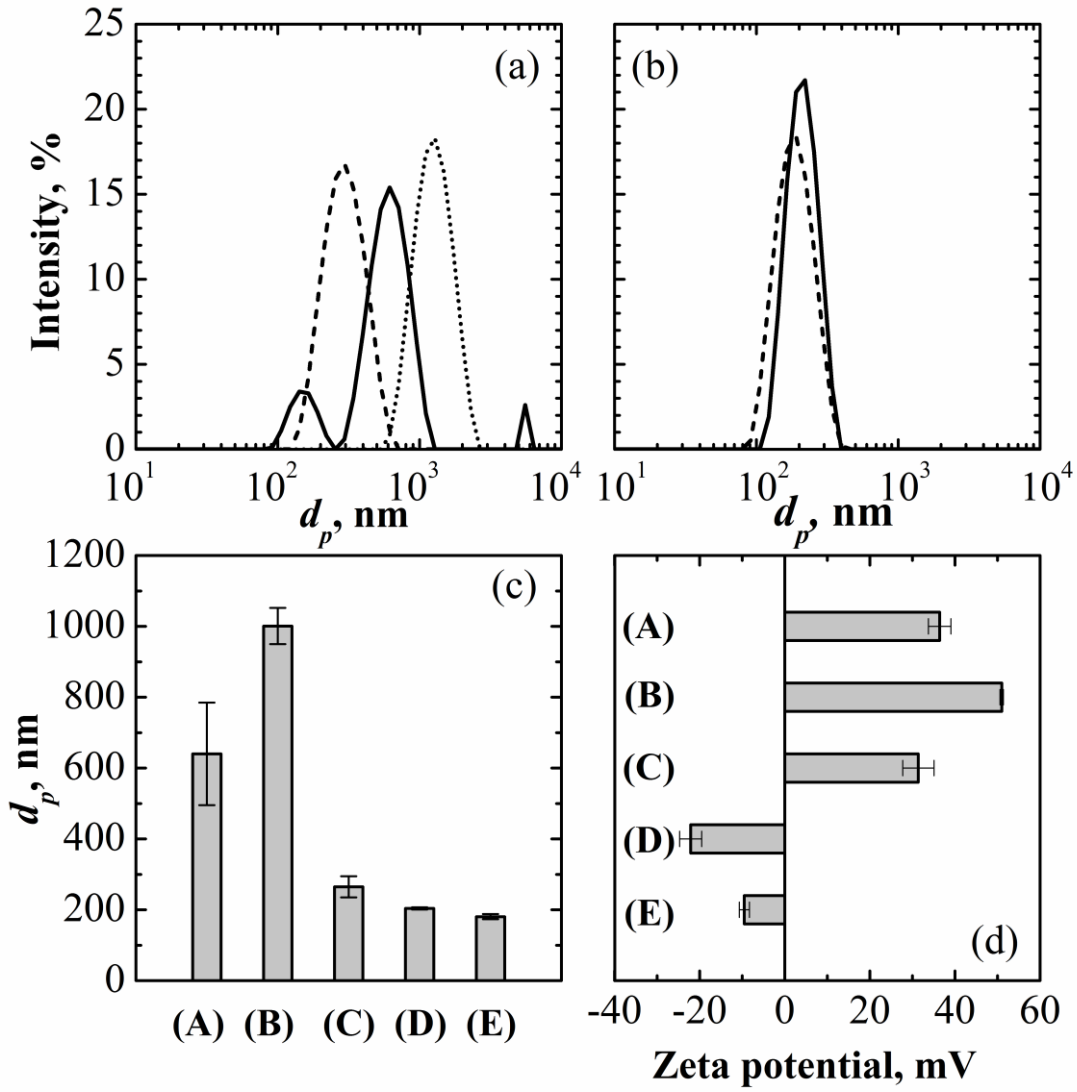

*Figure 3*

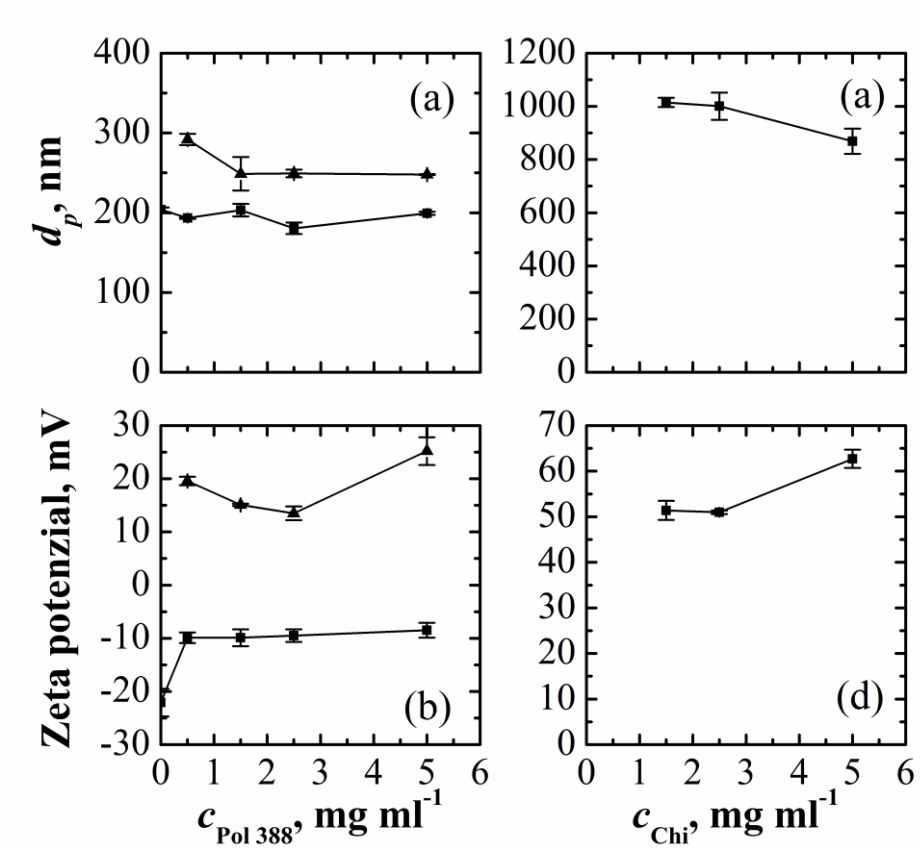

*Figure 4*

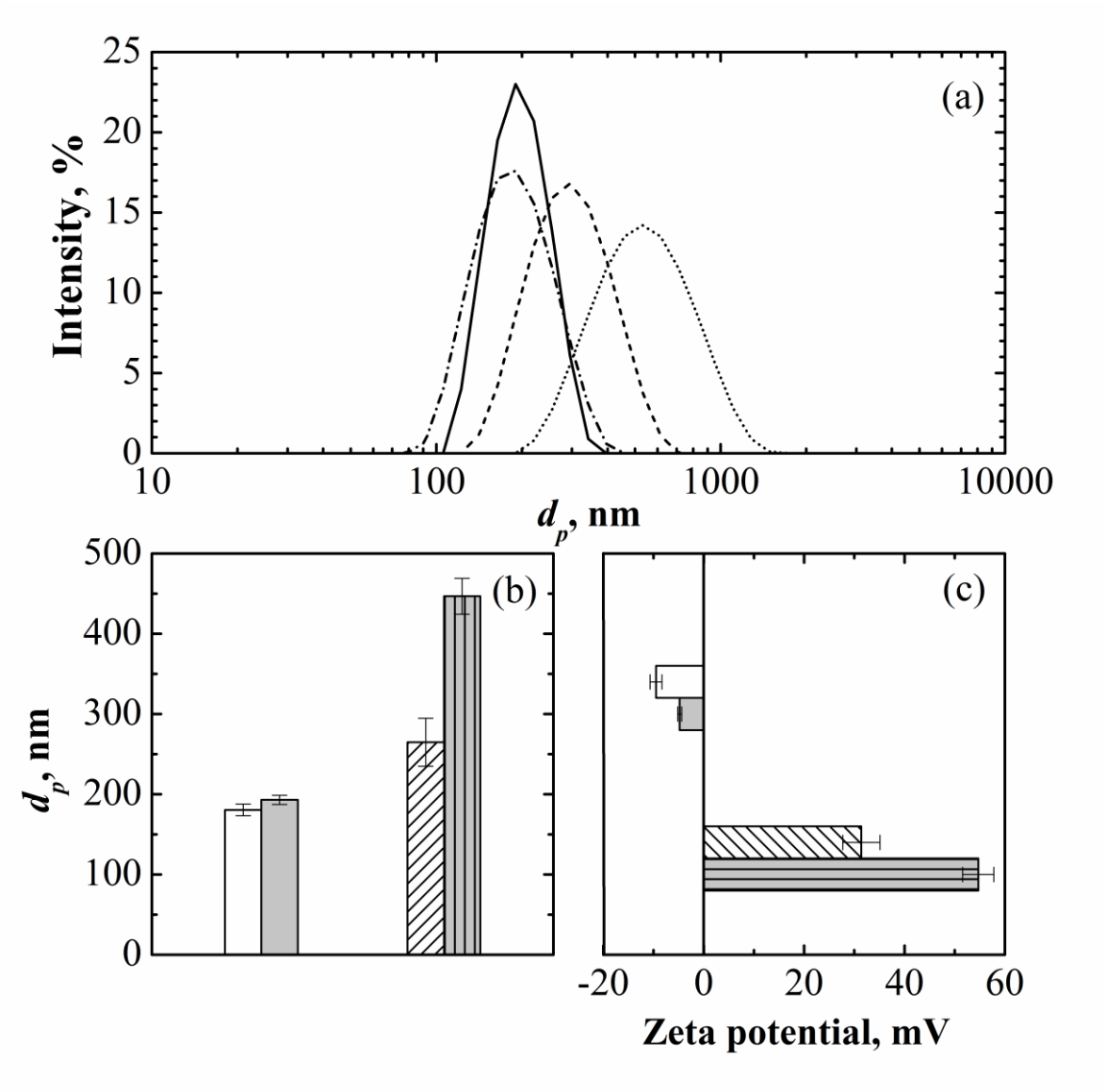
(a)
Intensity, %
25
20
15
10
5
0
10
100
1000
10000
$d_p$, nm
(b)
$d_p$, nm
500
400
300
200
100
0
(c)
-20
0
20
40
60
Zeta potential, mV

*Figure 5*

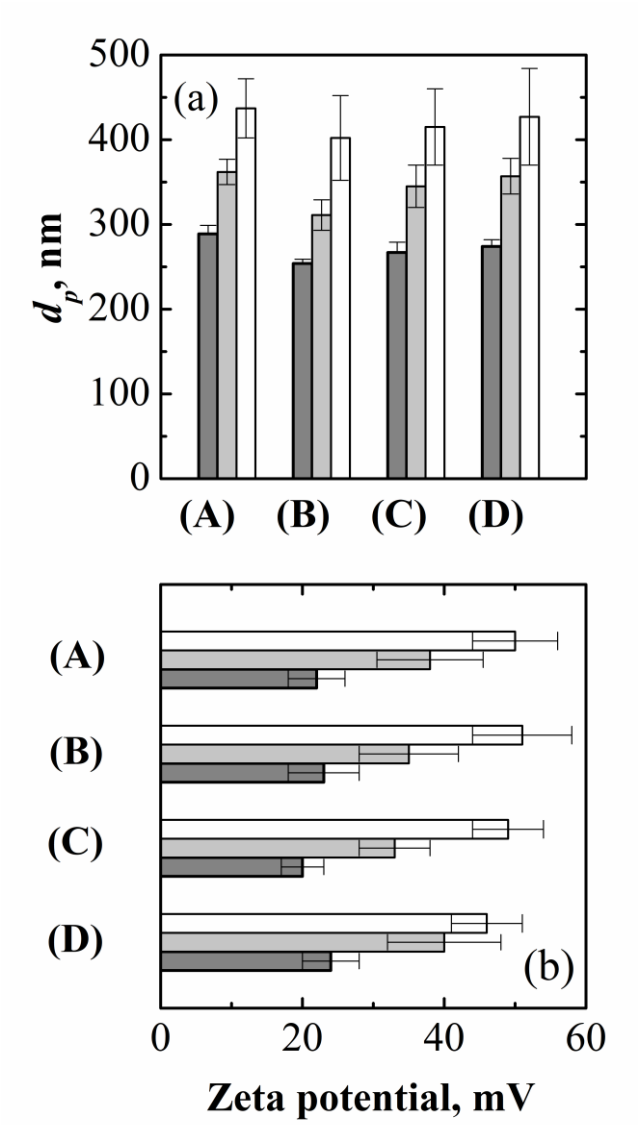
500
400
300
200
100
0
(a)
$d_p$, nm
(A)
(B)
(C)
(D)
(A)
(B)
(C)
(D)
(b)
0
20
40
60
Zeta potential, mV

*Figure 6*

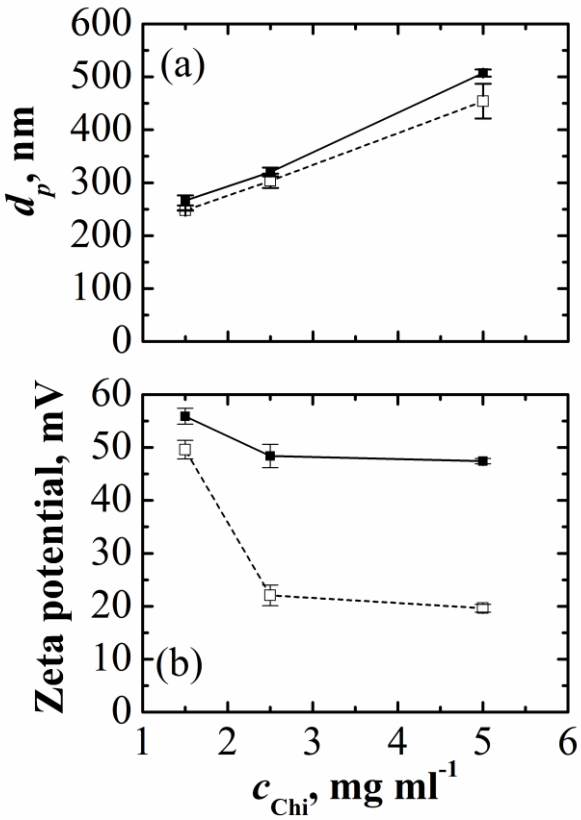
600
500
400
300
200
100
0
(a)
$d_p$, nm
60
50
40
30
20
10
0
(b)
Zeta potential, mV
1
2
3
4
5
6
$c_{Chi}$, mg ml$^{-1}$

*Figure 7*

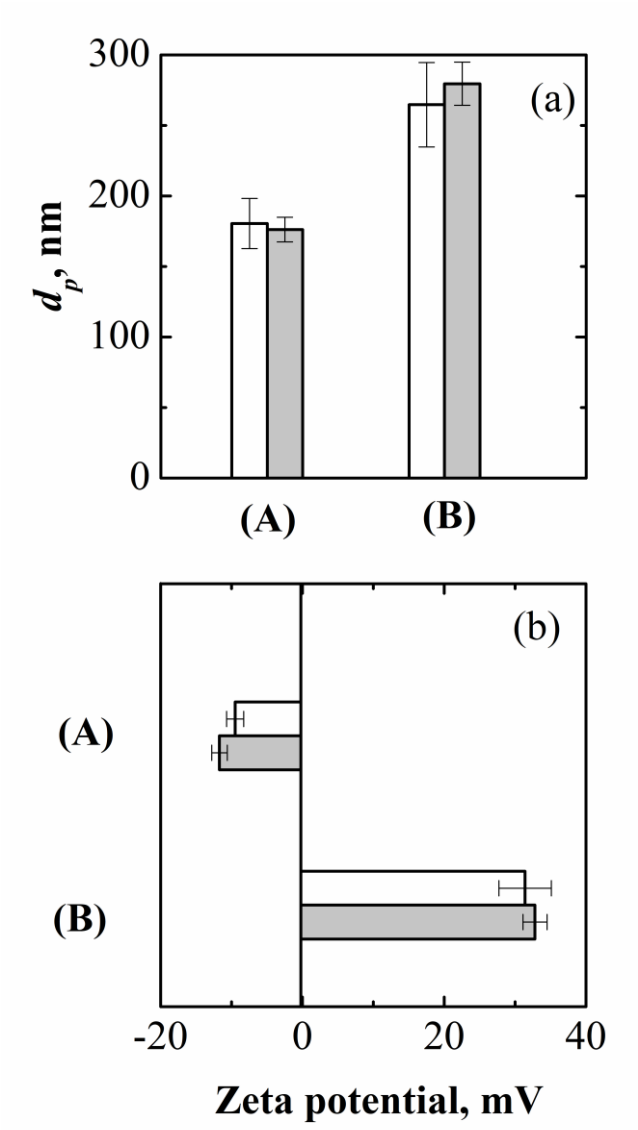

*Figure 8*

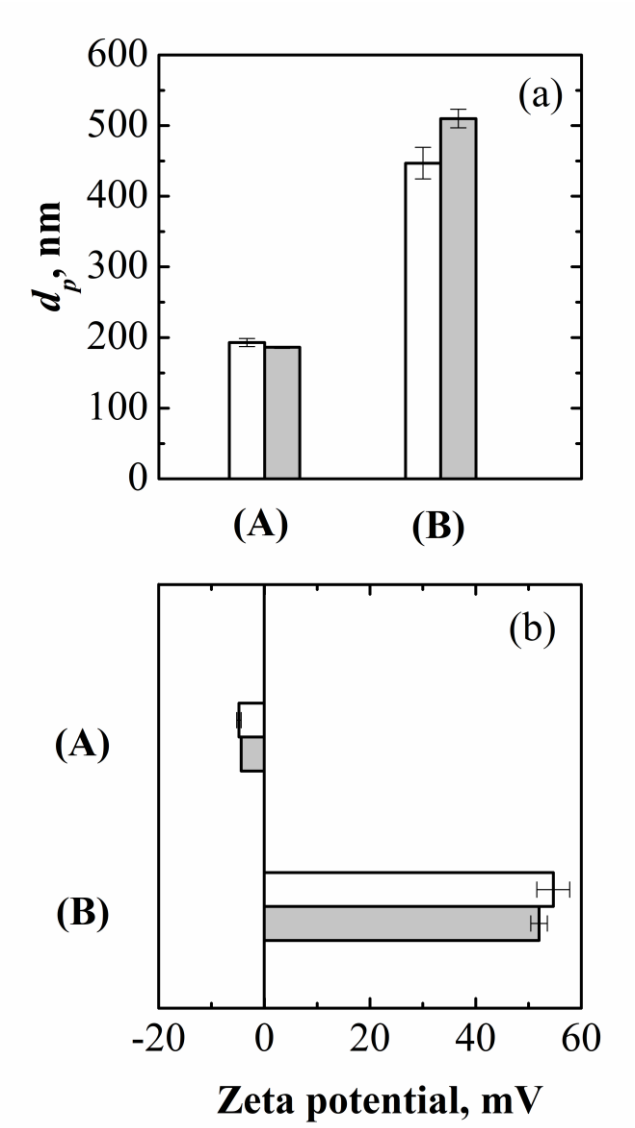
600
500
400
300
200
100
0
(a)
$d_p$, nm
(A)
(B)
(b)
(A)
(B)
-20
0
20
40
60
Zeta potential, mV

*Figure 9*

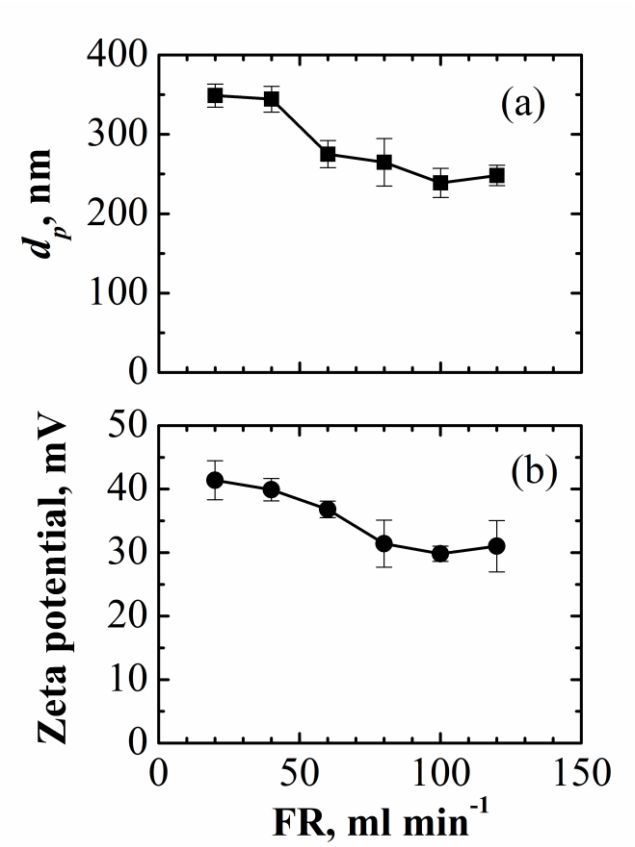
400
300
200
100
0
(a)
$d_p$, nm
50
40
30
20
10
0
(b)
Zeta potential, mV
0
50
100
150
FR, ml min$^{-1}$

*Figure 10*

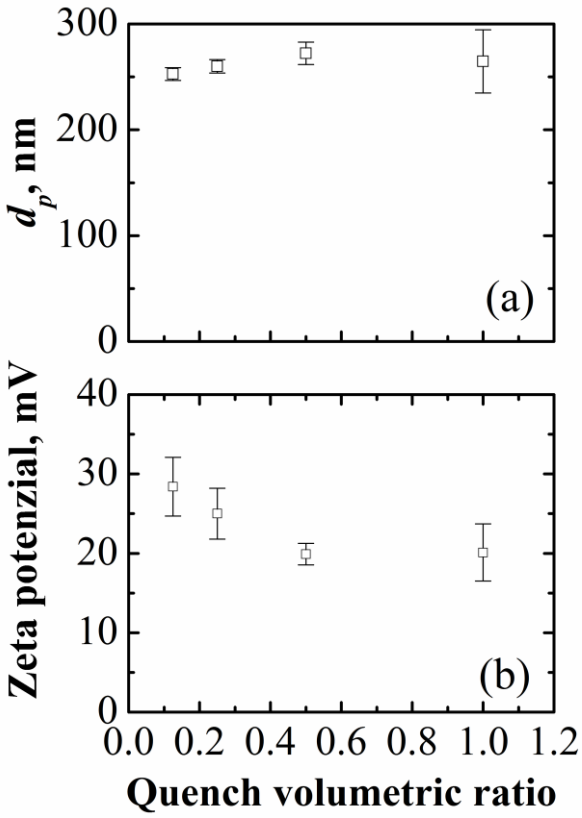
300
200
100
0
$d_p$, nm
(a)
40
30
20
10
0
Zeta potenzial, mV
(b)
0.0 0.2 0.4 0.6 0.8 1.0 1.2
Quench volumetric ratio